# FROM SINGLE- TO MULTI-TOWER SOLAR THERMAL POWER PLANTS: INVESTIGATION OF THE THERMO-ECONOMIC OPTIMUM TRANSITION SIZE

**Germain Augsburger[1] and Daniel Favrat[1]**

[1] Industrial Energy Systems Laboratory, Swiss Federal Institute of Technology, 1015 Lausanne, Switzerland

Phone: +41-(0)-21-693-5968, Fax: +41-(0)-21-693-3502, E-Mail: germain.augsburger@epfl.ch

## Abstract

When considering very large single-tower heliostat fields, the attenuation and spillage losses are growing with the distance to the central receiver. Therefore multi-tower configurations are modelled and investigated to find the thermo-economic optimal size of transition from single-to multi-tower plants.

First a method of building a multi-tower layout is defined, second a criterion is set up to select which receiver an individual heliostat is instantaneously aiming at, and third the thermo-economic performance of a three-towers heliostat field is compared to that of an equivalent single-tower heliostat field. Subsequently, a sensitivity analysis and a thermo-economic optimisation are performed both on single- and multi-tower configurations to find the two energy/cost trade-off curves and their intersection, which gives the thermo-economic optimum transition size from single- to multi-tower plants.

Keywords: solar tower thermal power plant, multi-tower, thermo-economic optimisation

## 1. Introduction

A multi-tower heliostat field features two towers or more with their respective receivers, whereat each heliostat can aim alternatively. Therefore the two main aspects of a multi-tower plant to investigate are the field layout and the heliostat aiming strategy. On the one hand, the field layout has to take into account the presence of one additional tower or more, without increasing the shading and blocking losses between neighbouring heliostats. On the other hand, the aiming strategy has to define a criterion to select the receiver whereat each heliostat is aiming instantaneously, e.g. by minimising the cosine, attenuation and spillage losses.

In this way, a multi-tower solar array (MTSA) was proposed by Schramek [1], where several grid-based heliostat fields are overlapping, and two to four towers are arranged in squares or triangles. This leads to a dense layout with small heliostats and towers (< 5 $m^2$, < 10 m) suited for urban areas, where the radiation unused by a conventional set-up is exploited by the mirrors inserted in-between the original rows. Then, given their distance to each tower, the heliostats are enabled to aim at a fixed number of receivers only, one up to four, whereon they are alternately directed. As a result, the amount of incident beam radiation hitting the ground can be captured by the field with a share of more than 85 % (annual ground area efficiency).

Similarly, a multi-receiver heliostat system architecture was patented by Caldwell [2], with the objective of increasing the heliostat and land utilisation efficiency for large fields and distributed receivers. Furthermore, by dynamically assigning the heliostats to the receivers the same way as previously, the cosine losses are reduced.

Since the land coverage of large solar tower plants in uninhabited areas remains a secondary issue and a minor cost driver, the two main objectives of the multi-tower layout presented here are the increase of the optical efficiency and the decrease of the specific costs (especially influenced by additional receivers). The layout is obtained by duplicating a single-tower circular layout, whose east and west borders are set by straight north-south lines. The duplicated layouts are assembled side-by-side along an east-west line, so that the duplicated towers are aligned as well. In addition to the common parameters of a single-tower circular layout ([3] with radial and azimuthal spacing), the distance between two towers is introduced as a decision variable. For the sake of simplicity, each tower is assigned the same height, although this also may be taken as a variable.

Figure 1 shows the field layouts for two, three and four towers, each featuring the same number of heliostats as the Gemasolar plant (2650 [4]). In this example, the distance between the towers is arbitrarily set at 750 m, 500 m and 375 m respectively. Increasing that distance up to the original west-east diameter would lead to a configuration that is equivalent to the layout of several separated smaller solar tower plants.

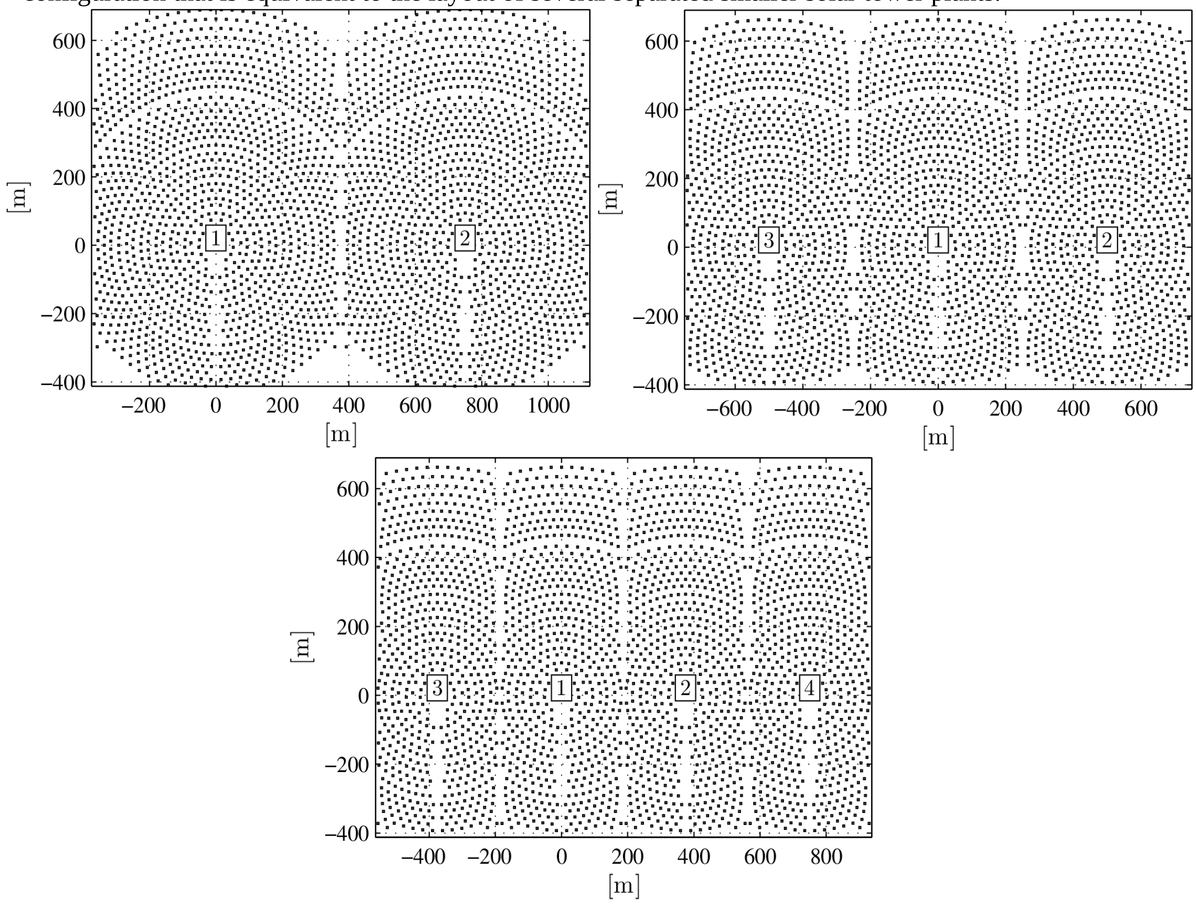


**Fig. 1. Multi-tower heliostat field layouts with two, three and four towers, and the same amount of heliostats as Gemasolar (2650 [4]).**

## 2. Aim selection criterion

Once the heliostats and the towers are laid out, the way the heliostats are aiming at the receivers has to be defined. First, the heliostats are not linked to one receiver permanently: each heliostat is assumed to be able to aim at any of the receivers at any time. Second, each single heliostat selects the receiver whereon its reflected radiation is the maximum at the given moment: the incident radiation that would hit the receiver surface is calculated for each of the three closest receivers separately, then the results are compared and sorted out, and finally the receiver with the highest amount of captured radiation is selected. Hence in other words, the receiver selection criterion is defined as the minimum optical loss occurring in the conversion of the incident radiation on the heliostat into the reflected beam captured by the receiver. This minimum loss criterion may include one, two or three of the following losses: the cosine loss, the atmospheric attenuation, and the spillage loss. Applying the cosine loss criterion ensures that the heliostat selects the receiver which involves an orientation with the minimum incidence angle on the mirror surface, and thus the maximum projected area in the aim direction. Subsequently, the atmospheric attenuation criterion allows to select the receiver direction where the reflected rays go through as less air mass as possible, to maximise the transmission. Then the spillage loss criterion leads to the selection of the receiver where the captured beam is the most concentrated, to minimise the radiation that misses the receiver surface.

The interest of applying the three loss criteria together is demonstrated in Table 1 by comparing the use of one, two or three of them. While the cosine criterion alone improves the field efficiency by 7 % with regard to the Gemasolar layout, the combination of the cosine and the attenuation criteria improves it by 17 %, and then by 32 % adding the spillage criterion.

Figure 2 shows the receiver selected by each heliostat on the spring equinox (March 20th) at ST 9:00, 12:00 and 15:00, for a three-tower layout with the same number of heliostats as Gemasolar (see Figure 1 on the right). The red arrow indicates the direction of the solar direct normal radiation. In the morning, the heliostats tend to aim at a receiver located on their east side, as the sun is still east and low in the sky hemisphere. As a result, the eastern receiver is selected by more heliostats than the two others, and its incident heat flux is the highest of all three, with a peak of 810 $kW_{th}/m^2$ (see Figure 2 on the right, in-house simulation [5,6,7]). The total thermal power reaches 155 $MW_{th}$. At noon, each heliostat obviously aims at its corresponding receiver according to the sub-field layout, and all three receivers are hit by the same flux distribution, achieving 190 $MW_{th}$. Then the situation in the afternoon is symmetric to that in the morning, with more heliostats for the western receiver.

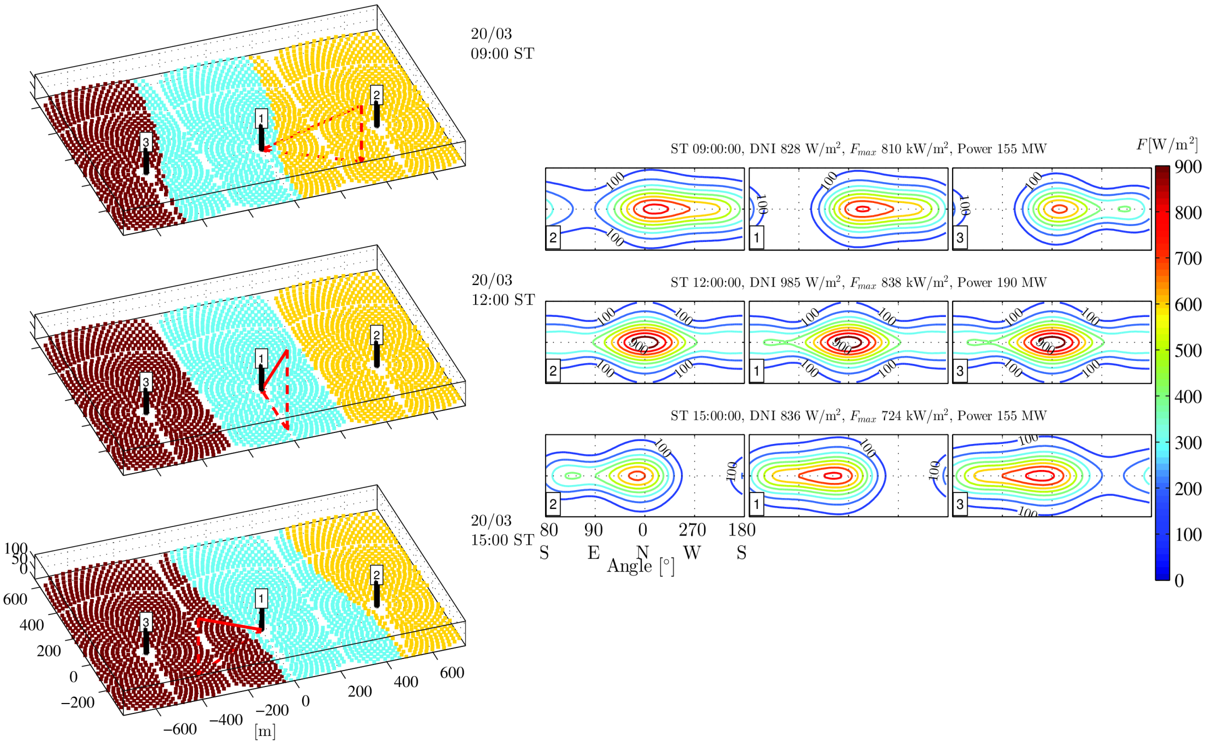


**Fig. 2. Aim selection by each heliostat and incident heat flux on the three cylindrical receivers of a multi-tower on the spring equinox (March 20th ) at ST 9:00, 12:00 and 15:00, based on the criterion of minimum cosine, attenuation and spillage losses (the direction of the sun is given by the red arrow).**

The efficiency of each heliostat is given in Figure 3, cumulated on the three specific days (spring equinox, winter and summer solstice). The heliostats located roughly between the two lines of y-coordinate -200 m and 400 m exceed the 50 % efficiency, whereas respectively below and above those lines the efficiency may fall down to 40 %. Thus this first multi-tower field layout presented here as example is clearly to be improved by varying the separation distance between the towers.

## 3. Multi-tower conversion cycle

The heat-to-power conversion cycles of the multi-tower plant are assumed to be independent from each other: each tower features its own PCU at its base. For the sake of consistency, the conversion technology is kept the same as that at the Gemasolar plant, based on a molten salt storage and a steam turbine. The solar multiple is also kept at the same high level of 2.8, allowing night operation.

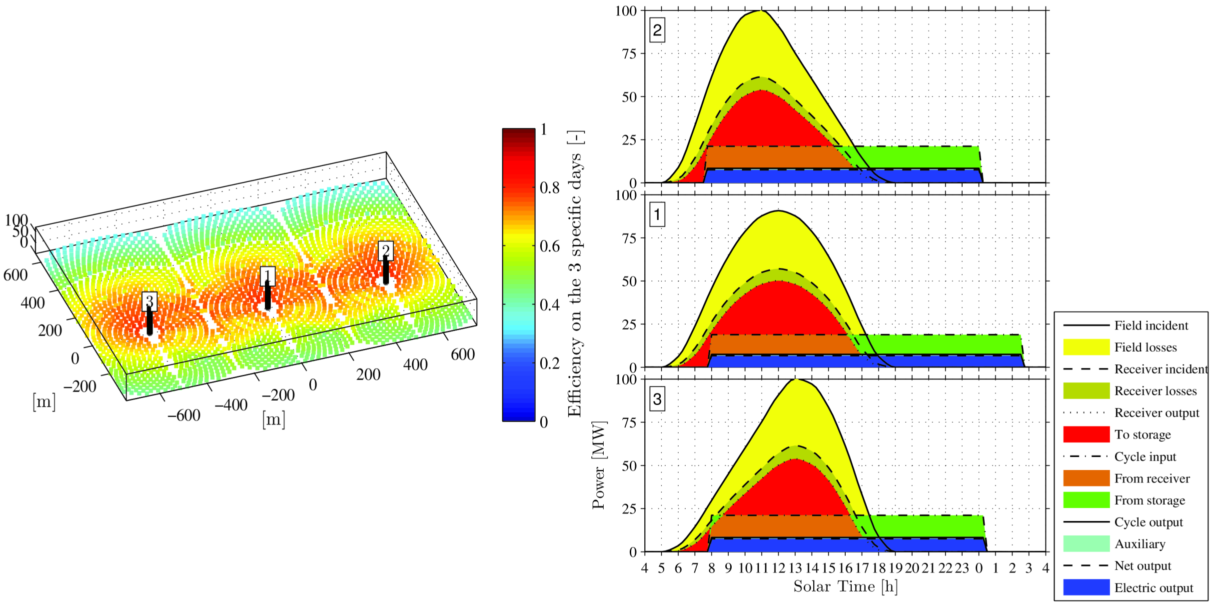


**Fig. 3. Calculated efficiency for the heliostats over the three specific days, and conversion cycle of each PCU in a three-tower plant on a perfect spring equinox (March 20th ), based on the same technology as Gemasolar (molten salt storage and steam turbine). .**

When simulating the cycle operation on a perfect spring equinox (March 20th), the east tower turns out to start slightly earlier than the two others (see Figure 3 on the right), due to the steeper increase in receiver power instantaneously caused by additional heliostats of the neighbouring field. Then the east receiver peak power of 54 $MW_{th}$ is achieved at ST 11:00, one hour before the middle receiver reaches its own peak at the lower value of 50 $MW_{th}$. In the afternoon, the east receiver power decreases linearly as more and more heliostats are defocusing to aim at the two other receivers. At the same time, the west receiver operates the other way around, increasing linearly in the morning, and achieving the same peak as the east receiver two hours later.

Now the exact same way as for the perfect equinox, the conversion cycle of every tower plant is simulated over the entire year based on the local DNI database. This results in the assessment of the respective annual electricity outputs, summing up to 114.6 $GWh_{el}$ in the current case, compared to the 87.5 $GWh_{el}$ of the simulated Gemasolar plant (pure solar).

## 4. Single- versus multi-tower comparison case

In order to measure the improvement brought by the heliostats ability to aim at additional receivers, a case of comparison between a single-tower and a multi-tower field layout is presented. The Gemasolar configuration is taken as the reference for the single-tower layout, while the three-tower field shown in Figure 1 is kept as the multi-tower base case, with the same heliostat dimensions, number of heliostats, tower height, and receiver dimensions as Gemasolar. Moreover, the three-tower field is assessed in three successive situations by applying one, two or three of the aim selection criteria proposed previously.

| Number of receivers | 1 | 3 | 3 | 3 | |
|---|---|---|---|---|---|
| Criterion of aim selection | | cos. | cos.<br>atten. | cos.<br>atten.<br>spill. | |
| Annual field efficiency | 45.3 | 48.5 | 52.9 | 59.8 | [%] |
| Max. receiver incident power | 138.2 | 174.9 | 175.1 | 179.2 | [$MW_{th}$] |
| Investment cost | 150.5 | 244.7 | 246.1 | 256.6 | [M$] |
| Levelised electricity cost | 24.1 | 35.2 | 32.5 | 29.7 | [c/$kWh_{el}$] |

**Table 1. Comparison of the performance of a three-tower layout with that of the Gemasolar layout.**

First, the annual energy performance of each case is calculated, which provides among others the annual field efficiency and the maximal receiver incident thermal power as comparison tools (see Table 1). In the case where the cosine, the attenuation and the spillage criteria are applied, the efficiency improvement exceeds 14 points from 45.3 % for Gemasolar up to 59.8 % for the three-tower layout. In parallel, the receiver incident power rises by more than 40 $MW_{th}$ from 138.2 $MW_{th}$ up to 179.2 $MW_{th}$.

Second, the economic performance is estimated by calculating the respective equipment costs, as well as the plant funding over the entire lifetime. Two indicators are given in Table 6.1 for the comparison: the total investment cost in M$ and the levelised electricity cost in ¢/$kWh_{el}$. Thus mainly because of the additional receivers, the total cost increases by 70 % from 150.5 M$ up to 256.6 M$. At the same time, the LEC goes up by 23 % from 24.1 ¢/$kWh_{el}$ to 29.7 ¢/$kWh_{el}$. Thus if the project economic viability is assumed to be ensured when the LEC remains below the local feed-in tariff, the three-tower base case presented here is more likely to be ruled out according to these results. Therefore the multi-tower fields in general are to be investigated through a multi-objective optimisation, in such a way that the critical parameters are found where a multi-tower layout becomes better, both at the energy and economic levels.

## 5. Sensitivity analysis

In the following, a sensitivity analysis is led on the key parameters of a multi-tower set-up, so that their influence on the plant thermo-economic performance is identified. The analysis is performed on the same three-tower base case proposed previously, and is expected to highlight the potential improvements. First of all, the impact of the towers separation distance is investigated, secondly the number of towers. Every time both the energy and the economic performance indicators are plotted against the given multi-tower variable.

### *5.1 Towers separation distance*

The separation between neighbouring towers is hence first varied from 500 m to 1000 m with 50 m steps, every other parameters being fixed. As a result, the field annual efficiency rises from below 60 % up to a peak of 62.8 % at 750 m and then stabilises slightly below that maximum value (see Figure 4 on the top left). Similarly, the receiver thermal power and the annual net electricity increase and stabilise above 750 m, whereas the receiver flux peak goes down to 840 $kW_{th}/m^2$ since it gets progressively evenly spread between the three receivers. As a matter of fact, the critical value of 750 m corresponds to the appearance of three distinct circular layouts, but still differing from a set of single-tower layouts by the heliostats ability to select their aim.

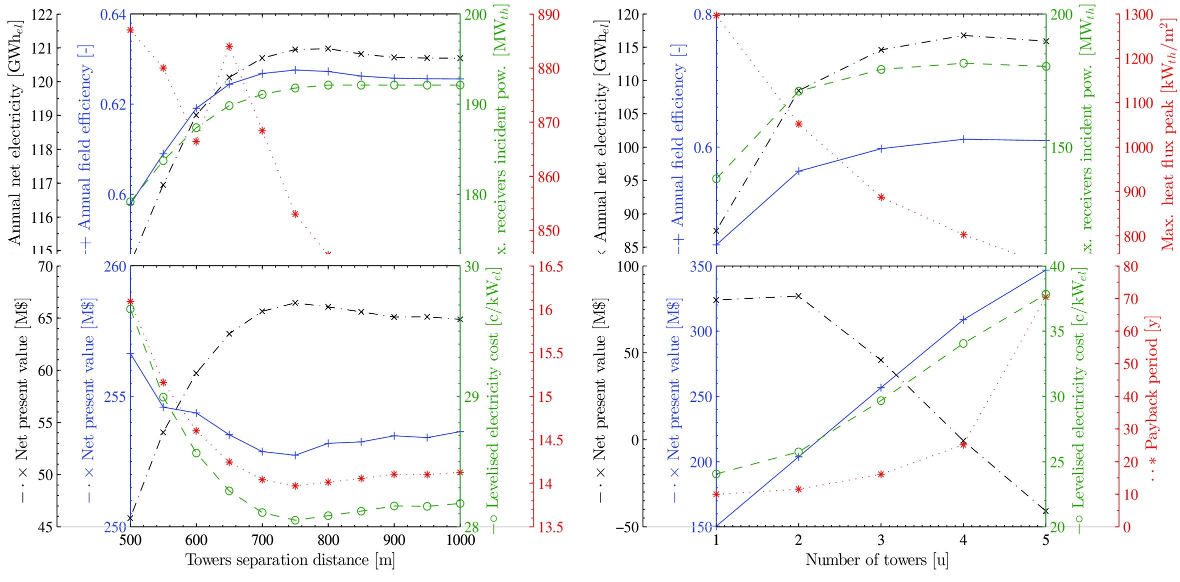


**Fig. 4. Sensitivity of the energy and economic performance to the towers separation distance and the number of towers, for a three-tower field with the same number of heliostats as Gemasolar (2650).**

Regarding the incidence on the economic performance (see Figure 4 on the bottom left), the total investment cost decreases slightly down to a minimum of 253 M$, mainly due to the decrease in storage costs. In parallel, the LEC also reaches a minimum of 28 ¢/kWhel at 750 m, as well as the payback period at 14 years, while the NPV peaks at 66.5 M$ and stagnates afterwards. That way, the variation of the separation distance shows here a match between the best energy and economic performances, both occurring around 750 m. As this is not necessarily the case for every decision variable, the influence of the number of towers is investigated in the following.

### *5.2 Number of towers*

Still keeping the number of heliostats constant at 2650, the number of towers ranges now from one to five, all featuring the same receiver. As expected, the field efficiency goes up significantly from 45.3 % with 1 tower to a maximum of 61.2 % with four towers, the same way as the receiver incident power and the electricity output, as shown in Figure 4 on the top right. At the same time, the receiver flux peak falls down from 1296 $kW_{th}/m^2$ to 735 $kW_{th}/m^2$, as it gets divided into the different targets.

Looking at the total investment, the number of towers has a large impact due to the costs of the additional receivers. Thus the investment grows almost linearly from 151 M$ up to 347 M$ for five towers. In a similar way, the LEC increases from 24.1 ¢/kWhel to 37.8 ¢/kWhel, as well as the payback period from 10 years to the prohibitive value of 70 years, while the NPV drops below 0 M$ beyond 4 towers. Therefore the number of towers turns out to be a variable that leads to contradictory energy and economic performances: there must be a trade-off between them.

### *5.3 Receiver area*

Given the impact of the receiver cost on the total investment, the receiver area may also be varied to identify potential efficiency improvements and cost reductions. Here the sensitivity of the three-tower layout is investigated for a receiver area that ranges from 1/4 to 3/2 of the Gemasolar case (251 $m^2$) with steps of 1/4. As a result, the annual field efficiency goes down to 35.8 % at 62.8 $m^2$, and reaches a ceiling around 63.6 % at 377 $m^2$. However, with this configuration the LEC shows no improvement, below as well as above 251 $m^2$, which seems to be already an optimum for the current three-tower field.

## 6. Thermo-economic optimisation of multi-tower plants

### *6.1 Multi-objective optimiser*

In order to find the multi-tower plant configurations that achieve both the best energy and economic performances, the use of a multi-objective optimiser (MOO) based on an evolutionary algorithm (EA) is proposed [8]. Hence the key parameters of a multi-tower plant have to be defined as decision variables, with a lower and upper limit of variation. In this way, the optimiser is able to randomly pick a value for each variable within the specified boundaries, and calculate the two objectives (investment cost in $ and electricity output in $Wh_{el}$) for this very first set of values. The MOO then repeats this operation until it reaches a given initial population of plants (e.g. 100 individuals). Subsequently, only the best individuals are kept: every individual that is worse than another in both objectives is eliminated. In other words, a plant set-up is left aside if any other plant set-up has both a lower investment cost and a higher electricity output. Based on this population of selected set-ups, some operations of crossover and mutation allows the creation of new individuals, and the operation of selection can be performed on the whole population once again. The entire process is repeated until the desired number of individual evaluations is reached (e.g. 5000 evaluations).

### *6.2 Multi-tower decision variables*

In the current case of multi-tower layouts, the decision variables include the same main single-tower parameters, and the two extra sensitivity variables presented previously: the heliostat width and height, the coefficient of spacing between successive rows, the south-to-north ratio (0: north field, 1: tower-centred), the number of heliostats, the towers height, the receivers diameter and height, as well as the towers separation distance and the number of towers. The boundaries of each decision variable is shown in Table 2: some extreme values such as the 1000 m tower height or the receiver dimensions of 100 m may sound unreasonable, but are necessary to ensure that the optimiser is searching for solutions in a large domain without being stuck by any variable.

### *6.3 Contradictory performance objectives*

Then the objectives have to be contradictory, otherwise if they are correlated the population of multi-tower plants degenerates into the single trivial solution of a mono-objective problem. As investigated in the previous sensitivity analysis, the energy and economic performances are expected to be contradictory: a more efficient plant turns out to be more costly, and vice versa, a cheaper plant is less efficient. Therefore the two objectives have to be an indicator of the energy performance on the one hand, and of the economic performance on the other hand: here the primitive indicator of each performance is taken, the total investment cost of the plant and its annual electricity output. Obviously the total investment cost is an objective to minimise, whereas the annual electricity output is to be maximised (see Table 2). In parallel, further objectives would be some derived indicators such as the plant efficiency and its LEC.

| *Decision variables* | Range | Unit |
|---|---|---|
| Heliostat width | 1-30 | [m] |
| Heliostat height | 1-30 | [m] |
| Radial spacing coefficient | 0-1 | [-] |
| South-to-north ratio | 0-1 | [-] |
| Number of heliostats | 100-100'000 | [u] |
| Towers height | 1-1'000 | [m] |
| Receivers diameter | 1-100 | [m] |
| Receivers height | 1-100 | [m] |
| Towers separation distance | 50-5'000 | [m] |
| Number of towers | 1-10 | [u] |
| *Contradictory objectives* | | |
| Total investment cost | min. | [$] |
| Annual electricity output | max. | [$Wh_{el}$] |
| *Constraints* | | |
| Receiver heat flux peak | < 1500 | [$kW_{th}/m^2$] |

**Table 2. Decision variables, contradictory objectives and constraints in the thermo-economic optimisation of a multi-tower plant.**

### *6.4 Constraints*

To narrow the domain of the objectives, or to avoid some damaging situations, one or more constraints may be added to the optimisation problem. By applying a strong penalty function to the plant set-ups that do not satisfy the constraints, extremely bad performances are artificially associated with them, and the optimiser eliminates them from the population. In the current case, the upper limit of 1500 $kW_{th}/m^2$ is put on the incident receiver heat flux peak, so that situations potentially leading to a receiver failure are restricted (e.g. materials fatigue, strong transients).

### *6.4 Pareto front of optimal trade-off multi-tower set-ups*

Following the MOO process described, a cloud of multi-tower set-ups appears with the creation of the initial population (see Figure 5). Then after a series of repeated selections, mutations and crossovers, a front of trade-off solutions starts shaping, narrowing and smoothing progressively. As the front converges towards what seems to be a limit, it stabilises and finding new set-ups that are equivalent or better than the others becomes more difficult. At this stage, the final Pareto front of optimal trade-off solutions is assumed to be achieved empirically, and there is no more need to perform additional evaluations. Since the optimiser here is seeking for minimum costs and maximum electricity output, the domain below the trade-off curve is considered as naive: all the multi-tower set-ups within this domain are worse than those on the curve. On the other hand, the domain above the trade-off curve is considered as infeasible: no multi-tower set-up can achieve any of the performances in this domain.

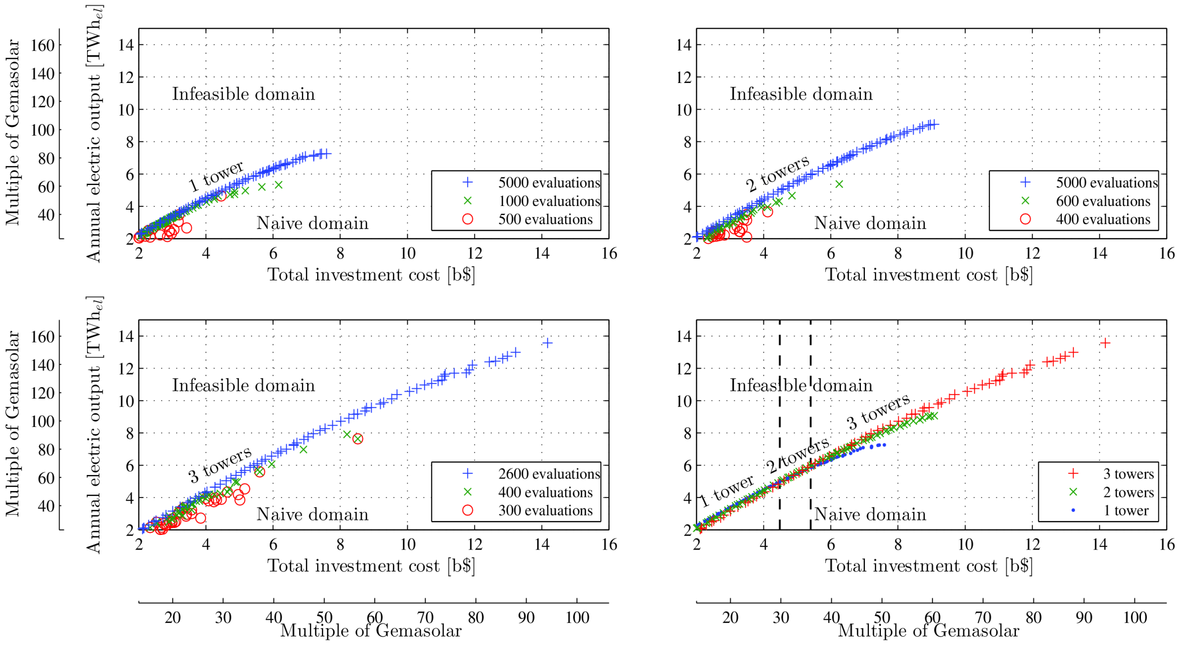


**Fig. 5. Pareto front of optimal trade-off one-tower, two-tower and three-tower set-ups.**

### *6.5 Optimum single- to multi-tower transition size*

When the three pareto fronts of respectively one-, two- and three-tower set-ups are superimposed (see Figure 5 bottom left), two intersection points appear and are indicated each by a vertical dashed line. The first intersection provides the transition from one- to two-tower set-ups at about 4.5 [b$] of total investment and an annual electric output of 5 [TWh$_{el}$], while the second gives the transition from two- to three tower set-ups at 5.4 [b$] and 6 [TWh$_{el}$]. For the sake of comparison, the first transition corresponds to 30 times the investment of Gemasolar and 57 times its electric output both estimated with the same model, and the second transition to 36 times and 68 times respectively. In terms of reflective area, the size of transition reaches 18 million square meter from one- to two-tower set-ups, and 20 million from two- to three-tower set-ups (Gemasolar has 318'000 [m$^2$]). For each transition the reflective area shows a significant drop when adding a tower, down to 16 and 18.6 million square meter respectively.

Table 3 shows the design parameters of the four transitions set-ups, as well as their energy and economic performances. Looking at the heliostat dimensions first, all of them feature a greater height than the width, with a ratio of roughly 1.5. Moreover, their values almost remain the same in all four cases, at around 13 [m] by 20 [m] which leads to a much larger area per unit than the nowadays most installed heliostats (e.g. 120 [m$^2$] at Gemasolar). Then the number of heliostats ranges from 60'000 up to nearly 80'000 units along the two successive transitions, while the towers separation distance gets closer to the limit of 5'000 [m] previously specified to the optimiser (see Table 2). In parallel, the dimensions of the tower and the receiver achieve very large values, above 600 [m] for the tower height and 60 [m] for the receiver diameter, which obviously is far beyond what is known from present-day existing plants, and thus is to be taken cautiously.

As a result of the additional receiver(s), the annual field efficiency rises from 0.46 with one tower to 0.52 with two towers in the first transition, and from 0.51 with two towers up to 0.53 with three towers in the second transition. Besides, the respective heat flux peaks remain as expected below the constraint of 1500 [kW$_{th}$/m$^2$]. Regarding the economic performance, all four cases show a similar levelised electricity cost slightly above 15 [¢/kWh$_{el}$], with a four-year payback period and a net present value between 8 [b$] and 11 [b$].

| | *Transitions* | | | | |
|---|---|---|---|---|---|
| *Design variables* | *1 to 2 towers* | | *2 to 3 towers* | | *Units* |
| Number of towers | 1 | 2 | 2 | 3 | [u] |
| Heliostat width | 12.49 | 13.26 | 13.33 | 13.23 | [m] |
| Heliostat height | 20.1 | 19.99 | 20.06 | 18.11 | [m] |
| Radial spacing coefficient | 0.26 | 0.37 | 0.38 | 0.38 | [-] |
| South-to-north ratio | 0.72 | 0.64 | 0.68 | 0.7 | [-] |
| Number of heliostats | 71328 | 60948 | 73122 | 77448 | [u] |
| Tower(s) height | 855 | 688 | 851 | 650 | [m] |
| Receiver(s) diameter | 93 | 76 | 78 | 68 | [m] |
| Receiver(s) height | 96 | 71 | 81 | 63 | [m] |
| Towers separation distance | 0 | 4863 | 4922 | 4565 | [m] |
| *Energy performance* | | | | | |
| Annual field efficiency | 0.46 | 0.52 | 0.51 | 0.53 | [-] |
| Max. receiver incident power | 8.14 | 8.24 | 9.81 | 9.74 | [$GW_{th}$] |
| Max. heat flux peak | 952 | 840 | 863 | 778 | [$kW_{th}/m^2$] |
| Annual field output | 16.43 | 16.66 | 19.75 | 19.77 | [$TWh_{th}$] |
| Nominal electric power | 0.92 | 0.95 | 1.14 | 1.11 | [$GW_{el}$] |
| Annual electric output | 4.98 | 5.03 | 5.96 | 5.98 | [$TWh_{el}$] |
| *Economic performance* | | | | | |
| Total investment costs | 4.48 | 4.53 | 5.4 | 5.43 | [b$] |
| Levelised electricity cost | 15.16 | 15.17 | 15.23 | 15.24 | [$c/kWh_{el}$] |
| Payback period | 4.16 | 4.17 | 4.2 | 4.2 | [y] |
| Net present value | 8.65 | 8.75 | 10.34 | 10.37 | [b$] |

**Table 3. Design variables, energy and economic performances of the optimal transition multi-tower set-ups from the pareto fronts.**

Figure 6 provides the four transition field layouts and the heliostats efficiency on a color scale from 0 to 1. At the first transition, the one-tower field shows heliostats whose efficiency exceeds 0.7 close to the tower, then remains greater than 0.5 until a 2'000 [m] distance thanks to the large receiver dimensions, but falls below 0.3 near the edge of the field. On the other hand, the two-tower field features two smaller sub-fields, whose edge heliostats are slightly better due to their shorter distance from the aim. Furthermore, the ability to select between the two receivers at any time results in better efficiencies at the middle field joint, up to 0.6 instead of 0.4. Subsequently at the second transition, while the two-tower layout looks similar to the latter one (except its slightly larger diameter), the three-tower layout has smaller individual diameters and also shows improved efficiencies at the two field joints. Along with the heliostats efficiency remaining now above 0.3 at the edge unlike the one-tower layout, this obviously leads to a higher overall field efficiency as presented in Table 3.

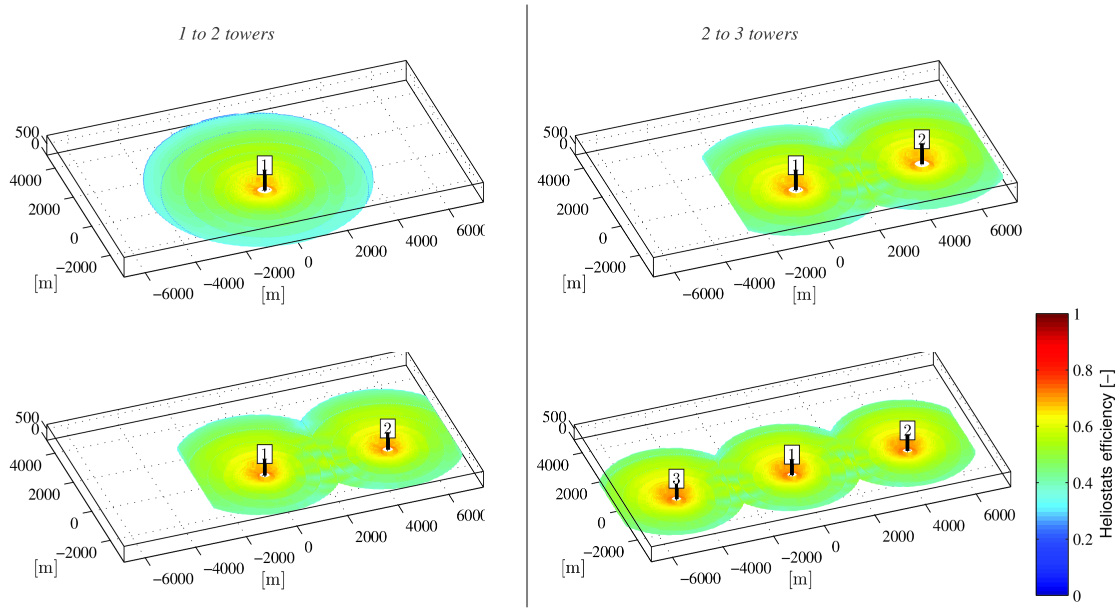


**Fig. 6. Heliostat field layout and efficiency of the optimal transition multi-tower set-ups from the trade-off pareto fronts.**

## 7. Conclusion

By envisaging very large heliostat fields for solar tower plants, the interest of creating multi-tower layouts has been identified, as the heliostat losses increase with the distance to the central receiver. Based on the combination of several one-tower fields, a simple layout generation has been presented with the example of two-, three- and four- tower layouts featuring the same amount of heliostats as the Gemasolar plant. Then, in order to decide at any time which receiver each heliostat is individually aiming at, a selection criterion has been proposed according to the instantaneous minimisation of the cosine, attenuation and spillage losses. In the base case of the Gemasolar-equivalent three-tower field, the application of the criterion allowed a 32\% increase in total field efficiency. Now regarding the power conversion cycle from the receiver to the electric generator, the assumption of a molten salt loop with a large storage system coupled to a steam turbine was made, and the multi-plant operation has been pictured throughout the day, showing slight power shifts between the three towers. After that, the one-tower reference plant was compared with its three-tower equivalent both at the energy and economic levels. Indeed, the energy performance of the multi-tower plant turned out to clearly exceed that of the one-tower plant, but at a much higher cost, which raised the need for an optimisation of the design parameters. This way, first a sensitivity analysis has been performed on the key multi-tower parameters, so that their influence on the plant thermo-economic performance of the plant could be highlighted, as well as the potential existence of optimum values. Second, the thermo-economic optimisation has resulted in a Pareto front of optimal trade-off set-ups for one-, two- and three-tower plants, eliminating naive solutions and converging towards the limit of feasibility. The optimal transition appears at a reflective area of 18 million square meter from one- to two-tower set-ups, and at 20 million square meter for two- to three-tower set-ups, which is respectively 57 and 63 times the size of Gemasolar. On the long-term perspective, this transition size might be reduced by significant improvements among the cost drivers such as the heliostats, the receiver, and the storage system.

## References

[1] Schramek, P., & Mills, D. R. (2003). Multi-tower solar array. Solar Energy, 75(3), 249–260.

[2] Caldwell, D. W. (2009). Multi-receiver heliostat system architecture.

[3] Siala, F. M. ., & Elayeb, M. . (2001). Mathematical formulation of a graphical method for a no-blocking heliostat field layout. Renewable Energy, 23(1), 77–92.

[4] Burgaleta, J. I., Arias, S., & Ramirez, D. (2011). GEMASOLAR, the First Tower Thermosolar Commercial Plant With Molten Salt Storage. Proceedings of the SolarPACES 2011 Conference on Concentrating Solar Power and Chemical Energy Systems. Granada, Spain.

[5] Augsburger, G., & Favrat, D. (2010). Thermo-economic Optimisation of the Heliostat Field of Solar Tower Thermal Power Plants. ecos 2010 - 23rd International Conference on Efficiency, Cost, Optimization, Simulation and Environmental Impact of Energy Systems (pp. 1–8). Lausanne, Switzerland: EPFL-LENI.

[6] Monterreal, R. (1998). New computer code for solar concentrating optics simulation. Proceedings of the 1998 9th SolarPaces International Symposium on Solar Thermal Concentrating Technologies, STCT 9; Font-Romeu; 22 June 1998 through 26 June 1998. Plataforma Solar de Almeria, Aptdo. 22, 04200 Tabernas, Spain.

[7] Collado, F. J., Gómez, A., & Turégano, J. A. (1986). An analytic function for the flux density due to sunlight reflected from a heliostat. Solar Energy, 37(3), 215–234.

[8] Molyneaux, A., Leyland, G., and Favrat, D. (2010). Environomic multi-objective optimisation of a district heating network considering centralized and decentralized heat pumps. Energy, 35(2):751–758.